A Prototype Three-Dimensional Position Sensitive CdZnTe Detector Array

Feng Zhang, Zhong He, *Senior Member, IEEE*, and Carolyn E. Seifert, *Member, IEEE*

***Abstract*—A new CdZnTe gamma-ray spectrometer system that employs two layers of modular detector arrays is being developed under the collaboration between the University of Michigan and the Pacific Northwest National Labaratory (PNNL). Each layer can accommodate up to three by three 3-dimensional position sensitive CdZnTe gamma-ray spectrometers. This array system is based on the newly developed VAS_UM/TAT4 ASIC readout electronics. Each of the nine detector modules consists of a pixellated CdZnTe detector and a VAS_UM/TAT4 ASIC front-end board. Each $1.5 \times 1.5 \times 1.0\ \mathrm{cm}^3$ CdZnTe detector employs an array of 11 by 11 pixellated anodes and a planar cathode. The energy depositions and 3-dimensional positions of individual interactions of each incident gamma ray can be obtained from pulse amplitude, location of each pixel anode and the drift time of electrons. Ten detectors were tested individually and half of them achieved resolution of $< 1.0\%$ FWHM at 662 keV for single-pixel events ($\sim 30\%$ of all 662 keV full energy deposition events). Two of them were tested in a simple array to verify that the upgrade to an array system does not sacrifice the performance of individual detectors. Experimental results of individual detectors and a two-detector array system are presented, and possible causes for several worse performing detectors are discussed.**

***Index Terms*—CdZnTe, detector array, gamma-ray spectrometer, position sensitive, three-dimensional (3-D).**

I. Introduction

TRULY HAND-HELD gamma-ray detectors with excellent energy resolution ($< 1.0\%$ FWHM at 662 keV), high efficiency and imaging capability are urgently needed for homeland security and nuclear non-proliferation applications. Mechanically cooled HPGe detectors are commercially available but are still too bulky to be called a "hand-held" device [1]. To date, the most promising candidates are still wide band-gap semiconductors, such as CdZnTe and $\mathrm{HgI_2}$. In the past ten years, several single-polarity charge-sensing techniques, such as coplanar-grid [2], Frisch-grid [3]–[5], or simple pixellated anodes [6], [7], have been developed successfully to mitigate the hole trapping problem and to improve energy resolution on larger volume CdZnTe and $\mathrm{HgI_2}$ detectors. However, material non-uniformity and electron trapping problems in these materials still limit the energy resolution of large volume (with an area about 2 cm^2 and a thickness about 1 cm) CdZnTe detectors to be worse than 2% FWHM at 662 keV.

Our approach to overcome the non-uniform detector response is the three-dimensional (3-D) position-sensing technique [8]. We read out signals from both the pixellated anodes and the cathode from which we can derive the deposited energy and 3-D coordinates of each individual gamma-ray interaction. Having the 3-D coordinates of each interaction, a correction for material non-uniformity and electron trapping in 3-dimensions becomes feasible. The first two generations of 3-D position-sensitive CdZnTe spectrometers were developed and reported in 1998 [9] and 2003 [10]. In 2004, we reported two 3-D position sensitive CdZnTe spectrometers coupled with the 3rd generation VAS3.1/TAT3 ASIC readout systems [11]. The CdZnTe detectors used in these two systems were $1.5 \times 1.5 \times 1.0\ \mathrm{cm}^3$ single crystals employing 11 by 11 pixellated anodes. Both systems achieved better than 1% FWHM resolution at 662 keV for single-pixel events and one system was even better than 0.8% FWHM. Other researchers are also exploring similar position-sensitive correction techniques [12], [13] for single-pixel events. The unique advantage of our device is its ability to fully reconstruct multiple gamma-ray interaction events (energies and 3-D coordinates) by measuring the electron drift times, which makes it possible to perform intelligent gamma-ray spectroscopy [14] and Compton imaging [15]. However, low efficiency due to the small sensitive volume (2.25 cm^3) limited their usage to laboratory demonstrations.

We are now developing the first truly hand-held 3-D position sensitive CdZnTe detector array. The upgrade in the ASIC and readout electronics from a single detector system to an expandable array system was done by Gamma-Medica-Ideas Inc. and was reported last year [16]. The most significant improvement from the previous single detector system is that the ASIC chip and the front-end board are miniaturized to closely match the size of the detector, thus multiple detector modules can be plugged on the motherboard to form an expandable detector array.

The goal of this project is to build a system in which multiple 3-D CdZnTe detector modules can be tiled together to achieve detection volume greater than 40 cm^3. This configuration allows the expansion of detector area to achieve higher detection efficiency while maintaining the excellent energy resolution ($< 1.0\%$ FWHM at 662 keV for single-pixel events).

II. System Description

A. Detector Module

The fundamental element of the array system is the detector module, which consists of an ASIC front-end board and a

Manuscript received January 15, 2007; revised May 21, 2007. This work was supported by the Department of Energy (DOE) NA-22 Office through the Pacific Northwest National Laboratory (PNNL), and the Department of Defense, Defense Threat Reduction Agency (DoD, DTRA).

F. Zhang and Z. He are with the Department of Nuclear Engineering and Radiological Sciences, University of Michigan, Ann Arbor, MI 48109 USA (e-mail: zhangf@umich.edu).

C. E. Seifert is with the Pacific Northwest National Laboratory, Richland, WA 99352 USA (e-mail: carolyn.seifert@pnl.gov).

Digital Object Identifier 10.1109/TNS.2007.902354

TABLE I
AVERAGE AND PIXEL MAP OF ENERGY RESOLUTION AND ELECTRON MOBILITY-LIFETIME PRODUCTS FOR TEN INDIVIDUAL DETECTORS

Detector Serial Number										
3E-1	3E-2	3E-3	3E-4	3E-5	3E-6	3E-7	3E-8	3E-9	3E-10	
Energy resolution of single-pixel events (FWHM at 662 keV)										2%
1.15%	0.77%	1.1%	1.04%	0.88%	0.95%	1.61%	0.98%	1.36%	0.96%	
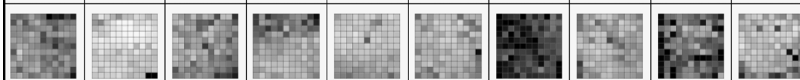										0.6%
Average and standard deviation of $(\mu\tau)_e$ ($\times 10^{-3}$ cm^2/V)										12.0
6.3 (1.3)	12.3 (0.8)	5.5 (0.9)	7.8 (1.4)	10.8 (0.7)	7.2 (1.5)	7.5 (2.3)	11.8 (1.2)	8.3 (3.5)	10.4 (1.1)	
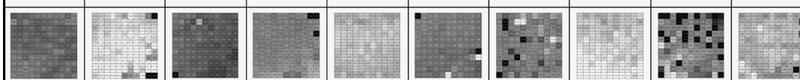										0.0
Correlation coefficients of energy resolution and $(\mu\tau)_e$										
-0.05	0.25	-0.3	-0.42	-0.26	0.1	0.0	0.14	0.13	-0.18	

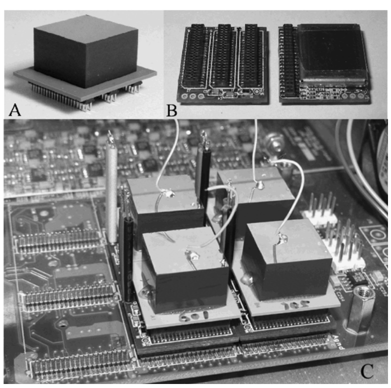

Fig. 1. Photos of the CdZnTe detector, the VAS_UM/TAT4 ASIC front-end boards and the detector array with four detector modules installed. (A) $1.5 \times 1.5 \times 1.0$ cm^3 CdZnTe crystal bonded on a ceramic substrate with three 42-pin 0.8 mm pitch pin connectors (from eV-PRODUCTS). (B) ASIC front-end board, three 42-pin 0.8 mm pitch socket connectors are used on the side facing the detector substrate, one 40-pin 1.0 mm pitch connector is on the side facing the motherboard, the 129 channel VAS_UM/TAT4 ASIC is enclosed inside the heat-sink. The area of each frond-end board is 2.2 by 2.2 cm^2. (C) Four detector modules are installed on the motherboard.

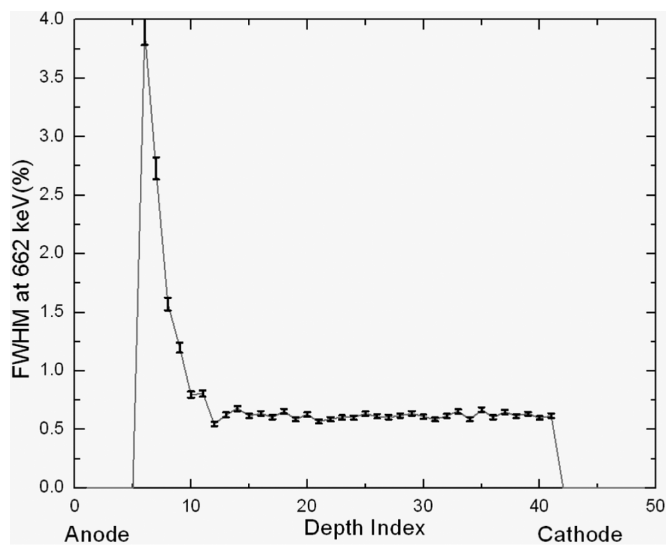

Fig. 2. Energy resolution (FWHM in %) versus depth index for one pixel.

$1.5 \times 1.5 \times 1.0$ cm^3 pixellated CdZnTe detector. The integration of 129 channels of energy-timing circuitries into one ASIC chip, which we named VAS_UM/TAT4, has made it possible to reduce the dimensions of the front-end board from about 4 by 6 inches in the old single detector system to 2.2×2.2 cm^2 in the new array system. Fine pitch connectors are used to couple the CdZnTe detector with the front-end board to form the detector module, and to connect the detector module to the motherboard. Pictures from the actual detector modules can be seen in Fig. 1.

B. Array Readout System

The array readout system mainly consists of a motherboard and a digital readout board. A FPGA on the motherboard controls all the ASICs. One digital readout board can synchronize signals read out from up to four motherboards for multi-layer operation. A National Instruments digital I/O board mounted inside a personal computer is used to communicate with the digital readout board [16].

Up to nine detector modules can be plugged into a motherboard and work as a single 3-D position sensitive CdZnTe imaging spectrometer with a sensitive volume up to 20.25 cm^3. Two layers of detector arrays will be operated together to achieve a detection volume of more than 40 cm^3 in the final handheld device.

III. EXPERIMENTAL RESULTS

We have received a total of ten $1.5 \times 1.5 \times 1.0$ cm^3 CdZnTe detectors from eV-PRODUCTS to date. These detectors were coupled with the ASIC front-end board, plugged in the motherboard and tested individually. Gamma-ray events ($\sim 5 \times 10^7$ events in $\sim$ 20 hours for each detector) from an uncollimated 10 $\mu\mathrm{Ci}^{137}\mathrm{Cs}$ point source 3 cm above the cathode were collected and used to calibrate the detectors. Data were collected under

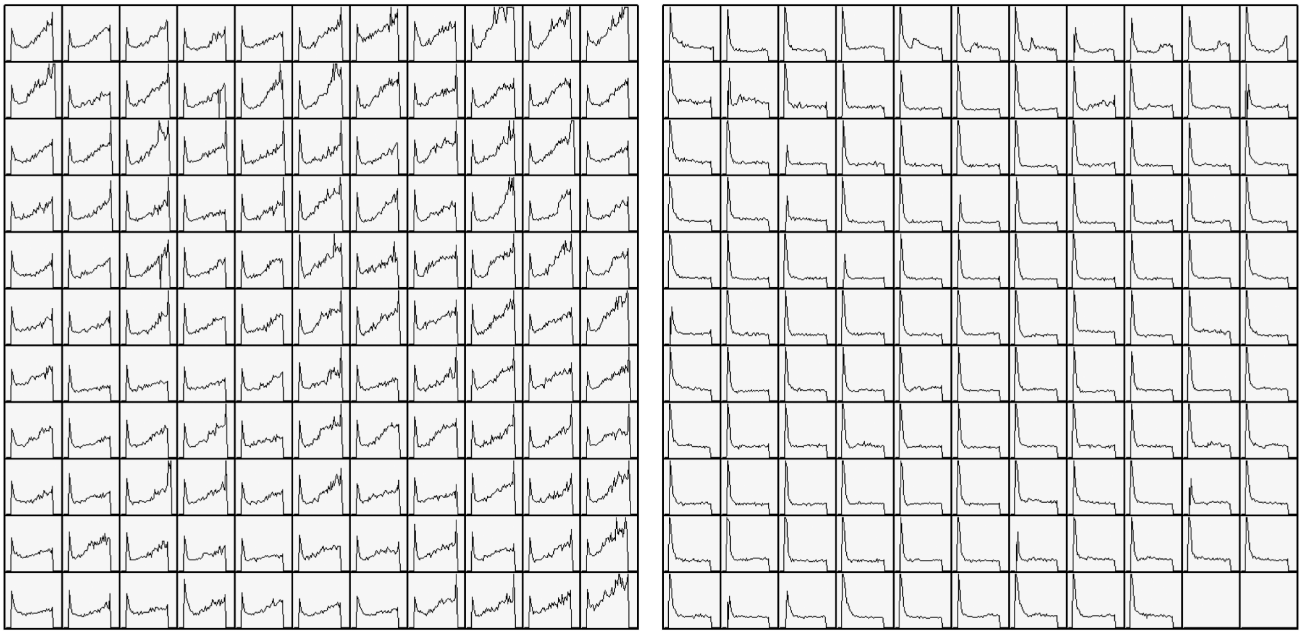

Fig. 3. Pixel maps of energy resolution (FWHM in %) versus depth index for detector #3E-1 (left) and #3E-2. Notes: There are two bad pixels on the lower-right corner of detector #3E-2.

different cathode biases to measure the electron mobility-lifetime products.

A. Individual Detector Performance

Table I shows energy resolution data of single-pixel events, electron mobility-lifetime data (average value and standard deviation of all pixels on each detector) and their pixel-pixel correlation coefficients ($(\overline{F \times \mu\tau} - \overline{F} \times \overline{\mu\tau})/\sigma_F\sigma_{\mu\tau}$; range from -1.0 to 1.0; a negative value means pixels having higher $(\mu\tau)_e$ also have better resolution) for all detectors.

All ten detectors meet our original specification of average $(\mu\tau)_e$ higher than $5 \times 10^{-3}\ \mathrm{cm}^2/\mathrm{V}$. In particular, detector #3E-2 has a high $(\mu\tau)_e$ of $1.2 \times 10^{-2}\ \mathrm{cm}^2/\mathrm{V}$ and achieved better than 0.8% FWHM energy resolution at 662 keV. This detector reproduced the energy resolution we achieved with one of the VAS3.1/TAT3 single detector system. However, some detectors with high $(\mu\tau)_e$ perform even worse than others. The correlation coefficients of the $(\mu\tau)_e$ and the energy resolution for all pixels on each detector shown in Table I could not provide any useful clue.

B. A Study of the Variations in Detector Performance

Having the ability to map each detector response in 3-D, we can study how the detector response change inside the detector [17]. Fig. 2 shows the relationship between the energy resolution and the interaction depth for one pixel. We can see the energy resolution remains almost constant over most of the thickness and degrades only very close to the anode due to rapid change of the weighting potential. This property is expected on a good working pixel.

However, from the pixel map of resolution versus depth for all pixels of two detectors shown in Fig. 3, we can clearly see most pixels of detector #3E-1 have degrading energy resolution towards the cathode side, in contrast to constant resolution over most depths on #3E-2.

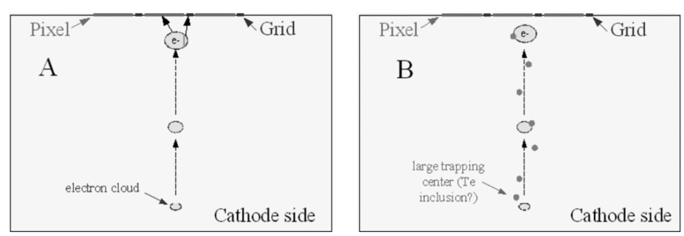

Fig. 4. Two possible causes of degrading energy resolution towards the cathode side. (A) Electron loss to the gap and the grid. (B) Electron trapping along the drift path due to large trapping centers.

There are two possible causes for degrading energy resolution towards the cathode side, as depicted in Fig. 4.

One possible cause is related to the final collection of electrons onto the anode. During the drift of the electron cloud from where it is created to the anode side, the size of the electron cloud continuously increases due to diffusion process. The final electron cloud arriving at the anode side may not be fully collected by one pixel and there may be some electrons trapped on the gap or collected by the anode grid. The electric field distribution in the region close to the anode can be quite different from detector to detector due to surface property variations and thus some detector may have much worse collection problems than others. The closer to the cathode that the electron cloud is created, the longer distance it drifts, and thus the larger is its size upon arriving at the anode. This could cause higher probability of and more variation in the electron loss to the gap and grid, thus poorer energy resolution towards the cathode side.

Another possible cause is electron trapping. If there are non-uniform large trapping centers (such as dislocation caused by Te inclusion [18], [19]) along the electron drift path, they can

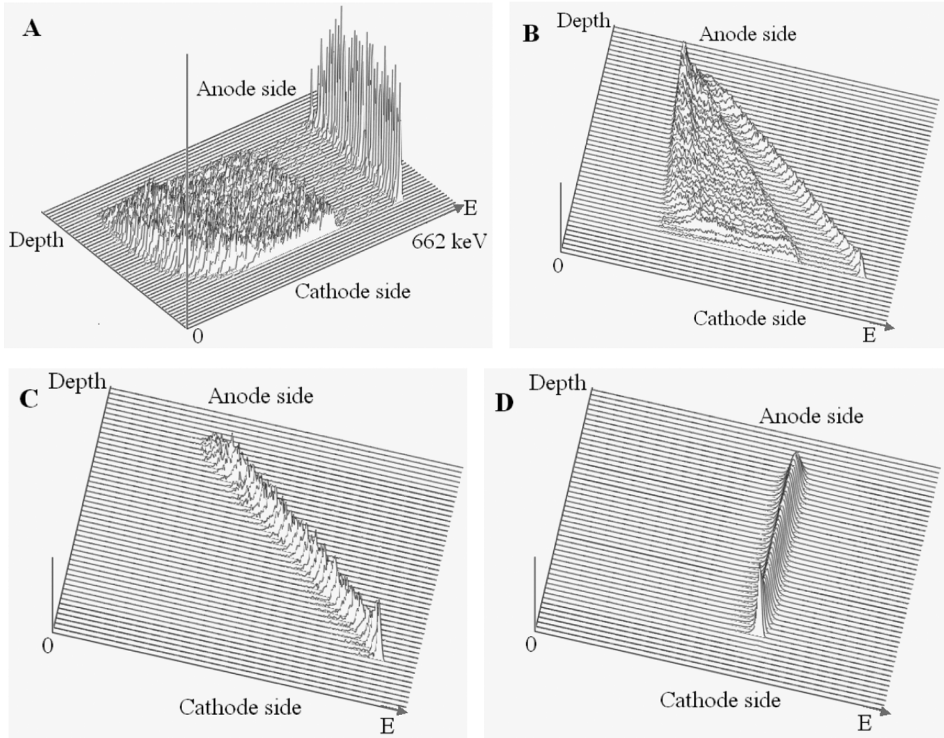

Fig. 5. (A) Depth separated spectra for a pixel. (B) Depth separated spectra for the cathode signal. (C) Photopeak region of depth separated cathode spectra. (D) Photopeak region of depth separated cathode spectra for all pixels aligned to the same centroid position.

cause larger fluctuation in electron trapping if electrons pass more trapping sites. It is evident that the longer the drift length, the larger the variation in electron loss due to trapping. As discussed in [17], 3-D position sensing and correction cannot improve such variations that are in a scale smaller than the pixel pitch.

It is impossible to tell from the anode signal which one of the above two caused the degrading resolution towards the cathode side, because the anode signal does not contain any information where the electrons are lost.

But the cathode signal is only affected by the second case since electrons trapped on the anode surface does not affect the cathode signal. Therefore a study in the cathode signal may reveal which cause degrades energy resolution.

For comparison, Fig. 5(a) shows depth separated spectra of a ^{137}Cs source for a pixel, while Fig. 5(b) shows depth separated cathode spectra for this same pixel. We can clearly see that the 662 keV photopeak position in the cathode spectra has a linear relationship with the interaction depth due to the linear weighting potential of the cathode. For each depth, we focus only on the photopeak region (cf. Fig. 5(c). First, align the photopeaks at the same depth for all anode pixels to the same centroid position (to increase counts in the peak and reduce statistical fluctuation), and then align all the photopeaks to the same centroid position [cf. Fig. 5(d)] to compare their shape from all depths.

Fig. 6 shows the aligned and normalized cathode spectra (photopeak region) for different depths. We can clearly see that the good detector (#3E-2) has consistent peak shape throughout all depths, while the worse detector (#3E-1) has increasing low energy tails towards the cathode side indicating the increased electron trapping. These results clearly reveal that the degrading energy resolution is due to fluctuations in electron trapping.

C. Array Performance

Due to higher-than-expected ASIC power consumption caused by a design flaw in the ASIC, the system runs hot with more than two detector modules plugged in. To be safe, we only tested two detectors (#3E-1 and #3E-2) in the array operation mode. The energy resolutions for individual detector modules and two modules as an array are listed in Table II. The "all-module" events mean the gamma rays interact in either one of the detector or both, while the "cross-module" events are those events in which gamma rays interact and deposit energies in both detectors.

For each individual detector in the two-detector array system, the energy resolutions are almost the same as when they were operated individually (only one detector plugged in the motherboard) and also similar to the results with the one-detector VAS3.1/TAT3 system [11]. This response shows that the migration from one-detector system to a multiple-detector array system is successful. As discussed in [11], the energy resolution degradation with increasing number of interactions is partly due to added electronic noise from multiple pixels and worse depth resolution from timing, but these factors cannot fully account for the degradation. Undetectable (below threshold) charge loss to the grid, the gap or neighboring pixels is a direction we are investigating.

For the array performance, we can see that the resolutions of all-module events are between the resolutions of each individual detector for the same type of events, as expected. However, the resolutions of the cross-module events (a few percent

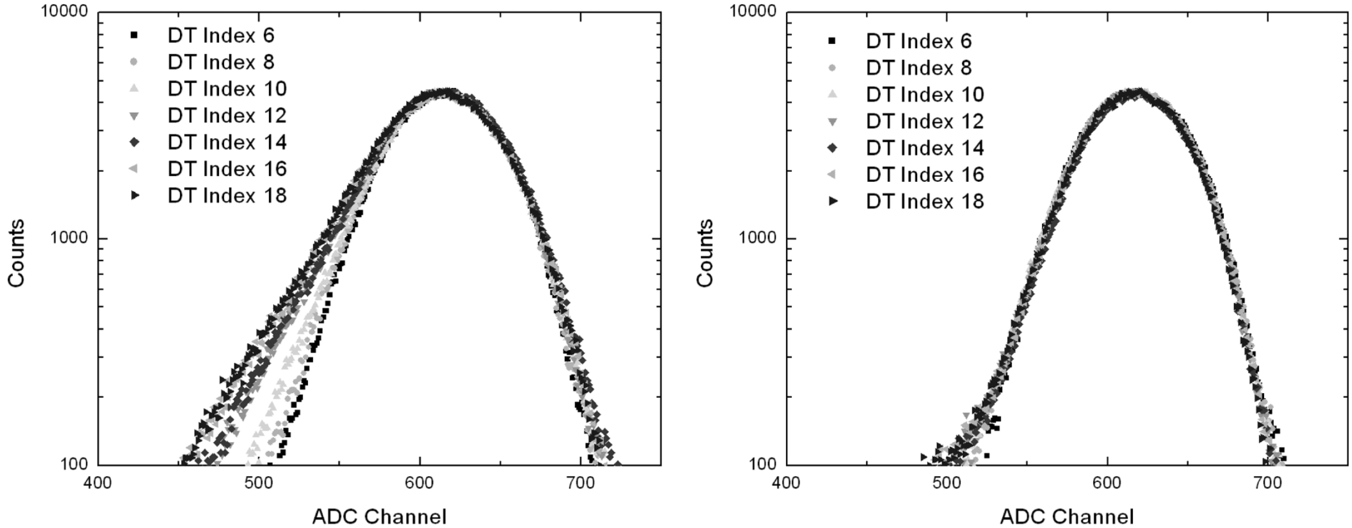

Fig. 6. Comparison of normalized and centered 662 keV photopeaks from the cathode spectra of different interaction depths derived from electron drift time for detector #3E-1 (left) and #3E-2 (right).

TABLE II
ENERGY RESOLUTION (FWHM AT 662 KEV) FOR INDIVIDUAL DETECTORS AND ARRAY WHEN TWO DETECTORS ARE OPERATED IN ARRAY MODE

	1-Pixel Events	2-Pixel Events	3-Pixel Events
#3E-1	1.15%	1.68%	2.12%
#3E-2	0.77%	1.18%	1.72%
All-module	0.89%	1.33%	1.88%
Cross-module		1.47%	2.18%

of all events) are worse than the all-module events of the same type. We are continuing our investigation on possible reasons.

IV. SUMMARY

A 3-D position sensitive CdZnTe detector array system using the VAS_UM/TAT4 ASIC readout electronics is under development. The design of the array system is based on the demonstrated single detector VAS3.1/TAT3 ASIC readout system while focusing on integrating the energy and timing circuits into a single chip, shrinking the size of the ASIC and the front-end board. The whole readout electronics have been designed to be scaleable. This means that multiple detector modules can be plugged in one motherboard to form a detector array, and multiple motherboards can be interconnected to achieve even higher efficiency without sacrificing the energy resolution.

The structure of the detector module and the basic configuration of the readout system are briefly introduced. Ten $1.5 \times 1.5 \times\ 1.0\ \mathrm{cm}^3$ CdZnTe detectors manufactured by eV-PRODUCTS have been tested individually with the new ASIC system. All detectors have electron mobility-lifetime products higher than $5 \times 10^{-3}\ \mathrm{cm}^2/\mathrm{V}$ with several detectors higher than $10^{-2}\ \mathrm{cm}^2/\mathrm{V}$. One detector produced better than 0.8% FWHM energy resolution at 662 keV for single-pixel events. However, we also observed that some detectors with quite high $(\mu\tau)_e$ do not perform very well. Our study clearly showed the degradation in energy resolution is mainly due to large fluctuations in electron trapping that cannot be fully compensated by 3-D correction.

Due to limitations in current system, only two detector modules were tested in array operation mode. The array operation preserved the good energy resolution of the two individual detectors for most part except that the cross-module events (only a few percent of all events) have worse than expected energy resolution. Upgrades to the current system, to achieve lower ASIC power consumption, lower energy threshold and better array operation performance, are underway.

REFERENCES

[1] Ortec_Inc. 801 South Illinois Ave., Oak Ridge, TN 37830.
[2] P. N. Luke, "Unipolar charge sensing with coplanar electrodes—Application to semiconductor detectors," *IEEE Trans. Nucl. Sci.*, vol. 42, pp. 207–213, 1995.
[3] D. S. McGregor, Z. He, H. A. Seifert, R. A. Rojeski, and D. K. Wehe, "CdZnTe semiconductor parallel strip Frisch grid radiation detectors," *IEEE Trans. Nucl. Sci.*, vol. 45, pp. 443–449, 1998.
[4] G. Montemont, M. Arques, L. Verger, and J. Rustique, "A capacitive Frisch grid structure for CdZnTe detectors," *IEEE Trans. Nucl. Sci.*, vol. 48, pp. 278–281, 2001.
[5] A. E. Bolotnikov, J. Baker, R. DeVito, J. Sandoval, and L. Szurbart, "HgI_2 detector with a virtual Frisch ring," *IEEE Trans. Nucl. Sci.*, vol. 52, pp. 468–472, 2005.
[6] H. H. Barrett, J. D. Eskin, and H. B. Barber, "Charge transport in arrays of semiconductor gamma-ray detectors," *Phys. Rev. Lett.*, vol. 75, pp. 156–159, 1995.
[7] J. E. Baciak and Z. He, "Spectroscopy on thick HgI_2 detectors: A comparison between planar and pixelated electrodes," *IEEE Trans. Nucl. Sci.*, vol. 50, pp. 1220–1224, 2003.
[8] Z. He, W. Li, G. F. Knoll, D. K. Wehe, J. E. Berry, and C. M. Stahle, "3-D position sensitive CdZnTe gamma-ray spectrometers," *Nucl. Instrum. Methods A*, vol. 422, pp. 173–178, 1999.
[9] W. Li, Z. He, G. F. Knoll, D. K. Wehe, and J. E. Berry, "A data acquisition and processing system for 3-D position sensitive CZT gamma-ray spectrometers," *IEEE Trans. Nucl. Sci.*, vol. 46, pp. 1989–1994, 1999.
[10] F. Zhang, Z. He, D. Xu, G. F. Knoll, D. K. Wehe, and J. E. Berry, "Improved resolution for 3D position sensitive CdZnTe spectrometers," *IEEE Trans. Nucl. Sci.*, vol. 51, pp. 2427–2431, 2004.
[11] F. Zhang, Z. He, G. F. Knoll, D. K. Wehe, and J. E. Berry, "3D position sensitive CdZnTe spectrometer performance using third generation VAS/TAT readout electronics," *IEEE Trans. Nucl. Sci.*, vol. 52, pp. 2009–2016, 2005.

[12] J. L. Matteson, R. T. Skelton, M. R. Pelling, S. Suchy, V. B. Cajipe, M. Clajus, S. Hayakawa, and T. O. Tumer, "CZT detectors read out with the RENA-2 ASIC," presented at the IEEE Nuclear Science Symp., Puerto Rico, Oct. 23-29, 2005.

[13] A. Shor, Y. Eisen, and I. Mardor, "Spectroscopy for Compton interaction in pixelated CdZnTe detectors," *IEEE Trans. Nucl. Sci.*, vol. 53, pp. 1656–1658, 2006.

[14] C. E. Lehner, Z. He, and G. F. Knoll, "Intelligent gamma-ray spectroscopy using 3-D position-sensitive detectors," *IEEE Trans. Nucl. Sci.*, vol. 50, pp. 1090–1097, 2003.

[15] C. E. Lehner, Z. He, and F. Zhang, "4π compton imaging using a 3-D position-sensitive CdZnTe detector via weighted list-mode maximum likelihood," *IEEE Trans. Nucl. Sci.*, vol. 51, pp. 1618–1624, 2004.

[16] F. Zhang and Z. He, "New readout electronics for 3-D position sensitive CdZnTe/HgI2 detector arrays," *IEEE Trans. Nucl. Sci.*, vol. 53, pp. 3021–3027, 2006.

[17] F. Zhang, Z. He, and D. Xu, "Analysis of detector response using 3-D position sensitive CZT gamma-ray spectrometers," *IEEE Trans. Nucl. Sci.*, vol. 51, pp. 3295–3299, 2004.

[18] S. A. Soldner, A. J. Narvett, D. E. Covalt, and C. Szeles, "Characterization of the charge transport uniformity of CdZnTe crystals for large-volume nuclear detector applications," *IEEE Trans. Nucl. Sci.*, vol. 51, pp. 2443–2447, 2004.

[19] M. Amman, J. S. Lee, and P. N. Luke, "Electron trapping nonuniformity in high-pressure-Bridgeman-grown CdZnTe," *J. Appl. Phys.*, vol. 92, pp. 3198–3206, 2002.